Distortion of ESD Generator Pulse Due to Limited Bandwidth of Verification Path

Janusz Baran and Jan Sroka, *Senior Member, IEEE*

***Abstract*—The paper deals with analysis of how limited bandwidth of a setup for verification of electrostatic discharge (ESD) generators affects reliability of testing. It is investigated how suppression of a high-frequency part of an ESD pulse spectrum distorts the pulse waveform and affects its standardized time domain metrics: the rise time and the peak value. Restriction of a pulse spectrum is achieved by low-pass filtering with a defined passband. The filtering models high-frequency attenuation of a measurement path, in particular that of an oscilloscope. The analysis is conducted for theoretical ESD pulses, specified by the IEC Standard, as well as for series of real noisy pulses recorded on setups with wideband 6 and 12 GHz oscilloscopes. Discrepancies of rise times and peak currents of filtered pulses with respect to an original input pulse are calculated as measures of distortion due to constraint of a pulse spectrum. It is shown that above 3 GHz, the setup circuit noise is the main factor contributing to measurement uncertainty of the metrics.**

***Index Terms*—Circuit noise, electrostatic discharges, frequency-domain analysis, uncertainty.**

I. Introduction

THE IEC Standard [1] deals with the human–metal electrostatic discharge (ESD). Such a discharge can take place when a charged person holding a pointed metal object, like a screwdriver or a ballpoint pen,[1] rapidly moves the hand against an electronic device (see Fig. 1).

According to the Standard [1], an idealized discharge current pulse can be described analytically using the formula

$$i(t) = \frac{I_1}{k_1}\frac{(t/\tau_1)^n}{1+(t/\tau_1)^n}e^{\frac{-t}{\tau_2}} + \frac{I_2}{k_2}\frac{(t/\tau_3)^n}{1+(t/\tau_3)^n}e^{\frac{-t}{\tau_4}}$$

$$k_1 = \exp\left[-\frac{\tau_1}{\tau_2}\left(\frac{n\tau_2}{\tau_1}\right)^{1/n}\right] \quad k_2 = \exp\left[-\frac{\tau_3}{\tau_4}\left(\frac{n\tau_4}{\tau_3}\right)^{1/n}\right] \tag{1}$$

with the following set of parameters: $\tau_1 = 1.1$ ns, $\tau_2 = 2$ ns, $\tau_3 = 12$ ns, $\tau_4 = 37$ ns, $I_1 = 16.6$ A, $I_2 = 9.3$ A, and $n = 1.8$ (values of I_1 and I_2 for 4-kV discharge voltage). We will name it the nominal pulse.

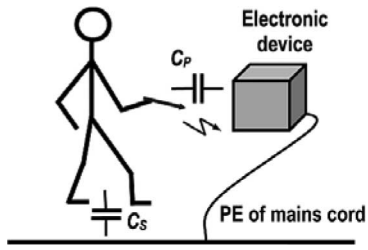

Fig. 1. Human–metal electrostatic discharge.

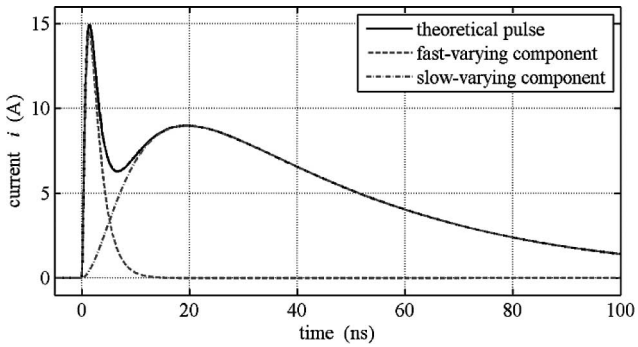

Fig. 2. Theoretical ESD current pulse and its components at 4 kV.

Two components of the current can be distinguished in the ESD phenomenon. The fast-varying component, represented by the first summand in (1) and the dashed line in Fig. 2, is due to arc discharge of a small capacitance C_p between the metal tip and the device. The slow-varying component, represented by the second summand in (1) and the dotted line in Fig. 2, results from discharge of a larger body capacitance C_s. The rise time of the nominal pulse (1) is equal to 0.8 ns.

The rise-time tolerance defined in Standard [1] is $\pm 25\%$. It means that, from the point of view of the required bandwidth, the worst case is a pulse with the shortest allowable 0.6 ns rise time, because its spectrum spreads out to higher frequencies. We will name it as the fast pulse. It can be modeled by (1) with $\tau_1 = 0.67$ ns, $\tau_2 = 2$ ns, $\tau_3 = 12$ ns, $\tau_4 = 37$ ns, $I_1 = 12.4$ A, $I_2 = 9.3$ A, and $n = 1.8$ (as before, I_1 and I_2 at 4 kV). Only τ_1 and I_1 change compared to the values for the nominal pulse. The fast pulse establishes the boundary of semirange of the rise-time variation for all acceptable pulses.

The waveforms and the power spectral densities (PSDs) of the theoretical nominal and fast pulse are shown in Fig. 3. The PSD of a signal is the squared magnitude of its Fourier transform.

Manuscript received April 25, 2010; revised July 11, 2010; accepted August 13, 2010. Date of publication September 23, 2010; date of current version November 17, 2010.

J. Baran is with the Institute of Electronics and Control Systems, Czestochowa University of Technology, Czestochowa 42–200, Poland (e-mail: baranj@el.pcz.czest.pl).

J. Sroka is with EMC-Testcenter Zurich AG, Zurich 8052, Switzerland. He is also with the Institute of Theoretical Electrical Engineering and Systems, Warsaw University of Technology, Warsaw 00–662, Poland (e-mail: j.sroka@emc-testcenter.com).

Digital Object Identifier 10.1109/TEMC.2010.2071386

[1]The test tip for air discharge in standard [1] is similar to the test probe for testing access to energized parts of an equipment under test, which is prescribed in low-voltage safety standards, e.g., [2]. Both are round. This is somewhat a contradiction between a real ESD phenomenon (pointed metallic object) and its representation in standard [1] (round metallic tip).

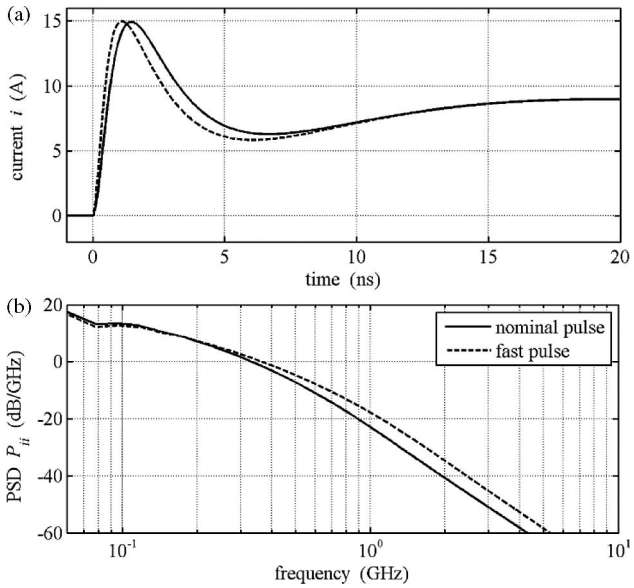

Fig. 3. Theoretical nominal (rise time $t_r = 0.8$ ns) and fast (rise time $t_r = 0.6$ ns) ESD pulse specified by Standard [1] at 4 kV: (a) waveforms; (b) PSD spectra.

For a sampled signal $x(n)$, it can be calculated as

$$P_{xx}(\omega) = \frac{1}{N}\left|\sum_{n=0}^{N-1} x(n)e^{-j\frac{\omega}{f_s}n}\right|^2 = \frac{1}{N}X(\omega)X^*(\omega) \qquad (2)$$

where $X(\omega)$ is the N-point fast Fourier transform (FFT) of $x(n)$, $X^*(\omega)$ is the complex conjugate of $X(\omega)$, and f_s is the sampling frequency. We have chosen the PSD, because it is the most common tool used in statistical signal analysis for description in the frequency domain. The PSD is a real positive function and has clear interpretation: power of a signal per unit frequency. The estimates of the PSD spectra were computed using the Welch method (MATLAB signal processing toolbox function `pwelch`): the total number of data samples ($N = 2000$ for 100-ns recording range and $f_s = 20$ GHz) was divided into four or eight overlapping segments, and the FFTs of the segments, windowed with the Hanning window to reduce effects of discontinuities at the segment ends, were averaged.

ESD pulses, formed by ESD guns (generators), are used for testing the immunity of electronic devices to electrostatic discharges. To ensure repeatability and reliability of the testing, generators have to be calibrated, especially in terms of standardized shape of the discharge current pulse. It is ruled by Standard [1]—the metrics of a gun discharge pulse that have to lie within limits allowed by the standard are: the rise time; the peak current; and the tail current after 30 and 60 ns.

Pulses of ESD guns are laboratory verified using a setup shown in Fig. 4(a), in the so-called "contact discharge mode," with the gun tip touching the inner disc of the target. The discharge current is initiated by closing contacts of a high-voltage switch in the generator output circuit [see Fig. 4(b)].

The answer to the question about necessary frequency bandwidth of a setup for verification of ESD guns has been changing over the recent decades. It began from 500 MHz in the middle

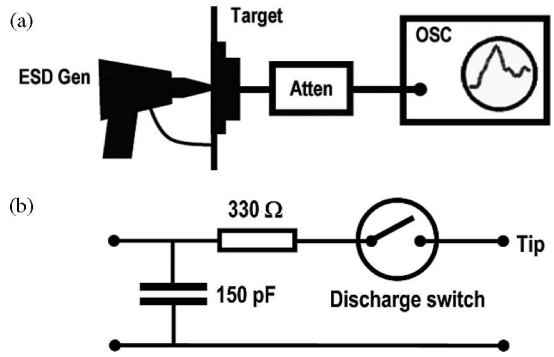

Fig. 4. Verification of an ESD generator. (a) Setup for ESD pulse measurement [3]. (b) Simplified diagram of the generator output circuit [1].

1980s of the 20th century. At that time, the rise time required by the standard had to be between 0.7 and 1.0 ns, so the bandwidth coincided with the rule of thumb determining the bandwidth depending on the pulse rise time $f_B = 1/(\pi \cdot 0.7\text{ ns}) \approx 460$ MHz. Then, in the middle 1990s, the required bandwidth was increased to 1 GHz and further to 2 GHz in the middle of the last decade. It is difficult to resist the impression that the answer has been dictated by capabilities of oscilloscopes available on the market at a given time.

The goal of this paper is to discuss more precisely the question: how wide should be the necessary bandwidth of a verification setup for distortion-free verification of an ESD gun? By "distortion-free" we understand capability of recording true time metrics of generated ESD pulses.

Estimation of the measurement uncertainty due to frequency-dependent distortions is costly, cumbersome [3], and increases budget. Therefore, information on whether verification can be considered as distortion-free or not is of very practical importance. If the frequency bandwidth of a setup is wide enough, the frequency-dependent distortion can be neglected. Consequently, only the accuracy of the low-frequency transfer impedance of a path, and vertical accuracy of an oscilloscope as well as its offset accuracy need to be taken into account in the measurement uncertainty of the peak value. Similarly, only the oscilloscope sampling rate and the peak value uncertainty need to be considered in the measurement uncertainty of the rise time. True rise time t_{true} can be roughly estimated from observed rise time t_{obs} using simple formula taking into account the oscilloscope lag: $t_{\text{true}} \cong \sqrt{t_{\text{obs}}^2 - t_{\text{osc}}^2}$, where t_{osc} is the rise time of the oscilloscope step response. As it was stated in [3] and [4], the aforementioned formula is valid only if the spectrum of the measured pulse lies within the oscilloscope bandwidth.

The limits of the expanded measurement uncertainty, recommended in Standard [1], are: $MU \leq 15\%$ for the rise time and $MU \leq 7\%$ for the peak value. We will assume that a setup with semirange of the time metrics variation ten times smaller than the expanded uncertainty recommended in [1] is distortion free.

Similar research on reconstructing an original ESD current from recorded data using frequency-dependent models of a measurement path are presented in [5] and [6].

II. Limitation of Spectrum of a Theoretical Pulse and Its Effect on Time Metrics

Low-pass filtering of an ESD waveform is a simple way to investigate how high-frequency damping of a verification path, first of all of an oscilloscope, affects the shape and the standardized metrics of the pulse in the time domain. The details of the output depend obviously on a type, and consequently, on frequency response of a particular filter. However, any selected filter should satisfy the following requirements: 1) filter order must be relatively high to reflect rapid roll-off of an oscilloscope frequency response above its passband [3]; and 2) filter phase response should be close to linear, as it is in the case of an oscilloscope input circuitry, to avoid strong distortion of an input waveform.

In this section, we show results of cutting off a high-frequency part of spectrum for theoretical waveforms defined by (1). For comparison, the computations were carried out for two low-pass filters: 1) Butterworth infinite impulse response (IIR) filter of order $N = 10$, chosen for its flat passband and relatively weakly nonlinear phase response; and 2) finite impulse response (FIR) filter of order $N = 50$, whose phase response is exactly linear. The order of a FIR filter must be much higher than that of an IIR filter to achieve comparable roll-off of their magnitude responses above a passband. Although IIR filters are more realistic models of analog systems, we chose a FIR filter to see difference between a linear and a nonlinear phase shift.

The nominal pulse ($t_r = 0.8$ ns) and the fast pulse ($t_r = 0.6$ ns) were filtered using the two selected low-pass filters, with the passband varying from 0.5 to 6 GHz. We determined rise times and peak values of filtered waveforms and compared them to those of the original unfiltered pulse calculating relative deviations

$$\delta_{\text{rise\_time}} = \frac{t_{r\_\text{filtered}} - t_{r\_\text{original}}}{t_{r\_\text{original}}} \tag{3a}$$

$$\delta_{\text{peak\_current}} = \frac{i_{\text{peak\_filtered}} - i_{\text{peak\_original}}}{i_{\text{peak\_original}}}. \tag{3b}$$

Deviations (3a) and (3b) represent uncertainties of a pulse metrics due to limited bandwidth of a measurement path. For the theoretical fast pulse, they are semiranges of variation of the metrics.

The bar graphs in Fig. 5 present deviations of the rise time and the peak current versus the pulse spectrum bandwidth for the two theoretical waveforms. One can see that when the spectrum is limited down to 1 GHz or below, the most visible distortion is increase of the rise time. For the 0.5-GHz bandwidth, it exceeds 90%. Unexpected effects of a raised pulse peak [$\delta_{\text{peak\_current}} > 0$, Fig. 5(b)] for narrow bandwidth Butterworth filtering, and in some cases, a steeper rising slope [$\delta_{\text{rise\_time}} < 0$, Fig. 5(a)] are caused by nonlinearity of the phase shift, which superimposes—in the time domain—spectral components of different frequencies.

Fig. 5 and Table I prove that the 3-GHz frequency bandwidth of a path is wide enough to ensure distortion-free transmission from a target to an oscilloscope memory (and display) in the worst case of the fast pulse. Semiranges of variations are ten times smaller then the expanded uncertainty specified in [1]. For the nominal pulse, even the 2-GHz bandwidth is sufficient.

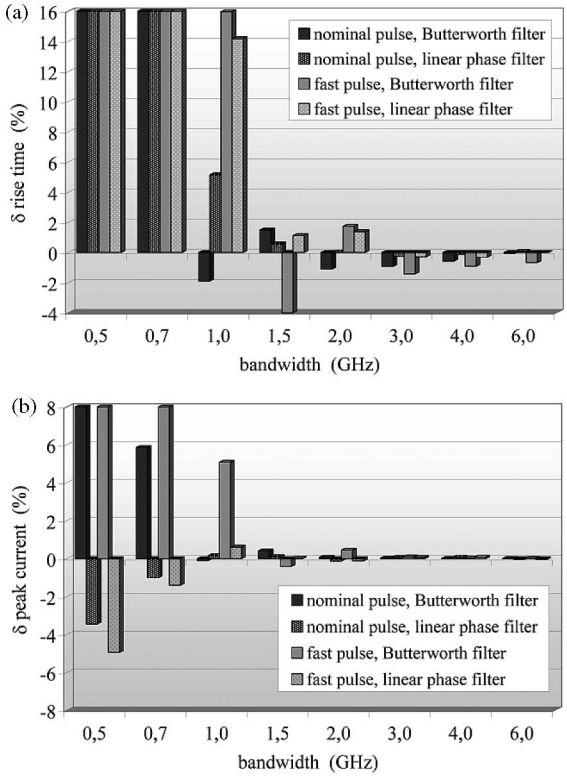

Fig. 5. Deviation of (a) rise time (vertical scale is clipped), and (b) peak current of theoretical pulses due to limitation of the spectrum bandwidth.

TABLE I
Relative Deviations of Time Metrics—Theoretical Pulses

	nominal pulse				fast pulse			
	Butterworth filter		linear phase filter		Butterworth filter		linear phase filter	
	2 GHz	3 GHz	2 GHz	3 GHz	2 GHz	3 GHz	2 GHz	3 GHz
$\delta_{\text{rise\_time}}$ (%)	-1.11	-0.93	0.02	-0.26	1.74	-1.43	1.38	-0.29
$\delta_{\text{peak\_cur}}$ (%)	0.07	0.03	-0.13	0.06	0.45	0.09	-0.12	0.06

III. Waveforms and Spectra of Measured ESD Pulses

This section deals with analysis of spectra of real ESD pulses recorded in guns verification. Fig. 6 shows waveforms generated in the same conditions by six different ESD guns. They were recorded on a setup consisting of a current target of 1.88-Ω resistance, a 20-dB attenuator, and a 6-GHz analog bandwidth, 20-Gsamples/s oscilloscope, for 1-kV discharge voltage [7]. The insertion loss of the target-attenuator-cable path was flat up to 4 GHz, as required in Standard [1].

Repeatability of pulses recorded for the same gun is quite good. It is illustrated in Fig. 7, which shows six pulses measured for one of the guns (we will name it gun 1), as well as power spectra of these waveforms.

For purposes of further comparisons, from now on we will be using normalized amplitudes of pulses, obtained after dividing

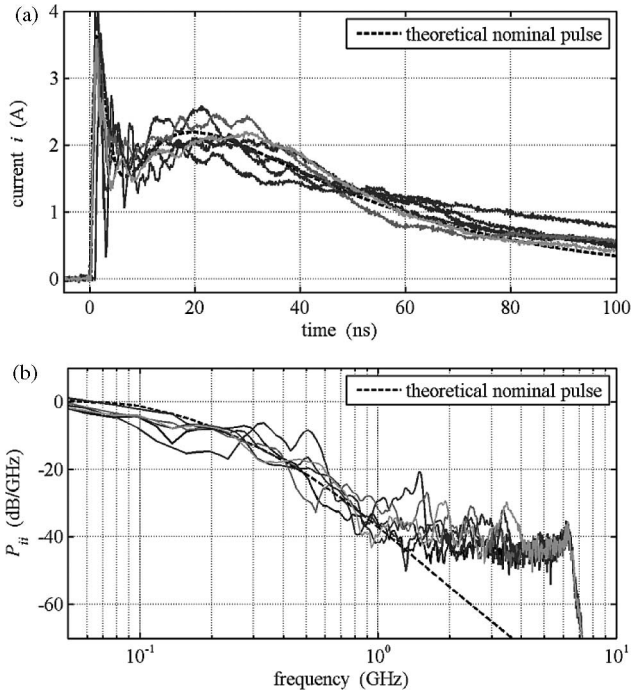

Fig. 6. ESD pulses recorded for six different guns at 1 kV: (a) waveforms; (b) PSD spectra.

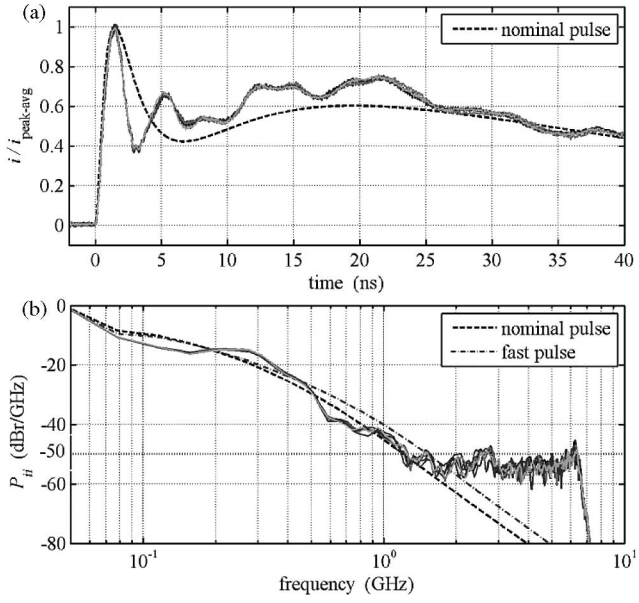

Fig. 7. Normalized ESD pulses of gun 1 (series of 6 measurements, 6-GHz oscilloscope bandwidth) along with theoretical approximations: (a) waveforms ($t_{r\_avg} = 0.86$ ns); (b) PSD spectra.

currents by a mean peak current of all measurements for a considered gun, so that the peak of a normalized current is about one. Consequently, the spectra in Fig. 7(b) are given in relative decibels (dBr) per GHz.

The spread of waveforms in Fig. 7(a) is small, comparable to the level of the measurement noise, which occurs also *prior to* start of the pulses. More distinctive details, common for all

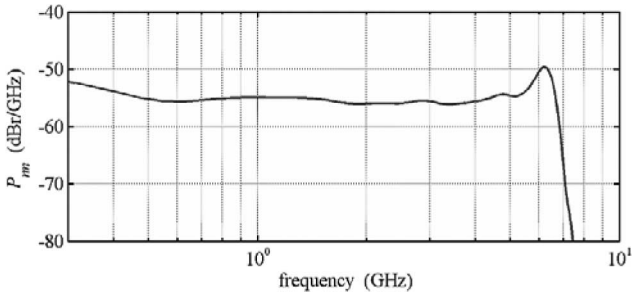

Fig. 8. PSD of measurement noise calculated for initial 10-ns interval prior to start of the pulses from Fig. 7.

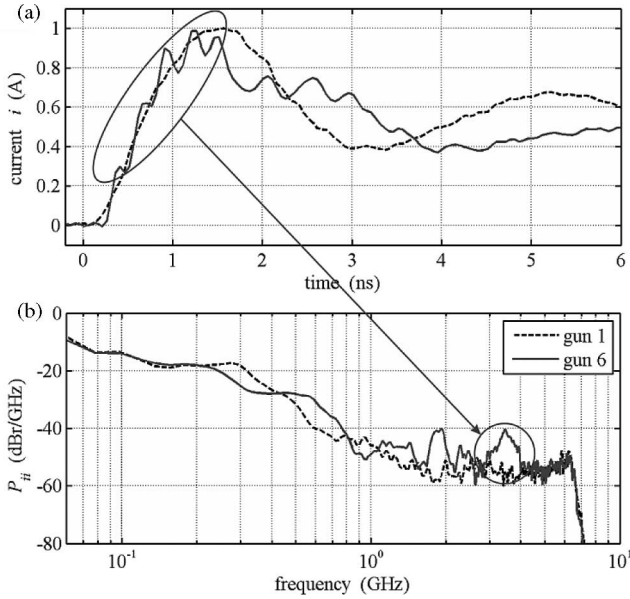

Fig. 9. Two normalized ESD pulses of different characteristics: (a) initial parts of waveforms; (b) PSD spectra.

waveforms, are not random. They can be treated as signatures characteristic for a particular gun.

The source of the wideband random noise present in the measurements is the gun, more precisely the output discharge switch—a high-voltage relay [see Fig. 4(b)]. This noise is transmitted trough the measurement path to the oscilloscope. Its spectrum P_{nn}, presented in Fig. 8, is approximately constant, at the level of -50 to -55 dBr/GHz over a wide range of frequency, up to about 6 GHz, i.e., up to the oscilloscope bandwidth. The spectrum in Fig. 8 is the average of spectra calculated for each measurement for the initial 10-ns interval of pure noise recorded prior to start of the discharge (only part of that interval is visible in Fig. 7(a) for $t < 0$).

From Fig. 6, we can see that details of a pulse, i.e., whether it is smooth and more similar or "rough" and less similar to a theoretical pulse, depend on a gun. It is better visible in Fig. 9, which compares initial parts of waveforms and spectra of two very different ESD pulses selected from those shown in Fig. 6. The pulse of gun 1 [one of those shown in Fig. 7(a)] is smooth and its spectrum above about 2 GHz is approximately flat and predominated by the noise. Almost the whole power of such a

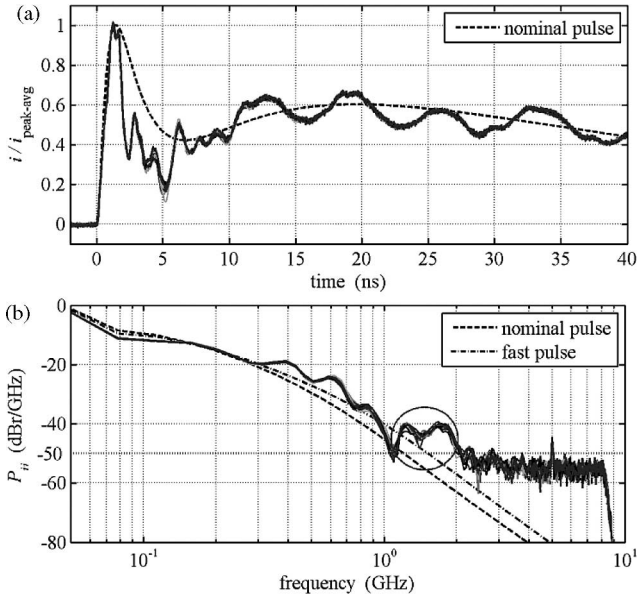

Fig. 10. Normalized ESD pulses of gun 2 (series of 10 measurements, 12-GHz oscilloscope bandwidth) along with theoretical approximations: (a) waveforms, $t_{r\_avg} = 0.85$ ns. (b) PSD spectra.

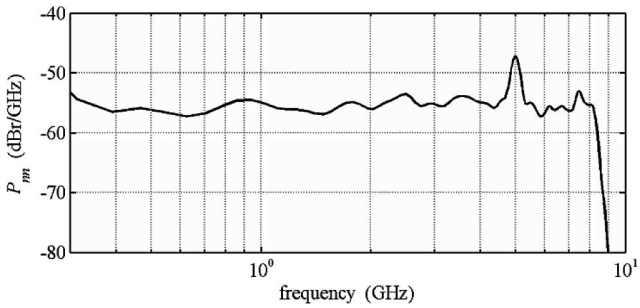

Fig. 11. PSD of measurement noise calculated for initial 10-ns interval prior to start of the pulses from Fig. 10.

pulse lies within the 2-GHz bandwidth. On the other hand, the pulse of gun 6 has a stepped rising slope and multiple small peaks, which translates into two resonant peaks standing out above the noise level in the high-frequency range of its spectrum. The resonance peak between 3 and 4 GHz, marked in Fig. 9(b), is associated with oscillations on the rising slope. For such a pulse, it can be even difficult to define unambiguously its rise time.

A series of ten ESD pulses, recorded for another gun (we will name it gun 2) on another setup with a 12-GHz analog bandwidth, 40-Gsamples/s oscilloscope, at 4-kV discharge voltage, is presented in Fig. 10 (for comparison the records were predecimated to $f_s = 20$ GHz). Again, repeatability of the measurements is good, and the noise, whose spectrum is shown in Fig. 11, is a wideband noise similar to that of gun 1.

The spectrum of the noise is limited to about 8 GHz due to damping of the target. It contains a professional N-7/16 connector, whose characteristic impedance (50 $\Omega \pm 1\%$) is guaranteed by the manufacturer up to 7.5 GHz.

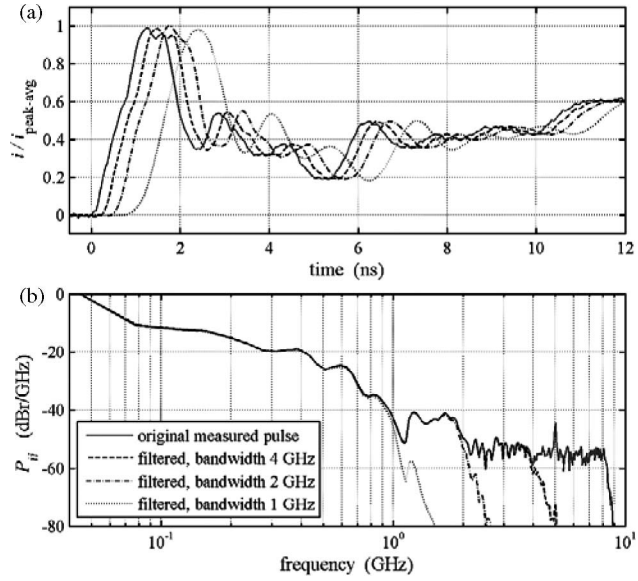

Fig. 12. Filtering of a single normalized gun 2 pulse with low-pass Butterworth filters of order $N = 10$: (a) time waveforms; (b) PSD spectra.

The pulses generated by gun 2 are not as smooth as the pulses of gun 1. In consequence, between 1 and 2 GHz, their spectrum emerges clearly above the level of the noise and above the spectra of the theoretical pulses [area in circle in Fig. 10(b)]. The peak of the noise spectrum at 5 GHz in Fig. 11 is most probably due to resonance of the target (frequency response of an oscilloscope within its bandwidth must definitely be flat). Such resonance is acceptable, because, as we mentioned earlier, Standard [1] does not specifies parameters of a verification path above 4 GHz.

The fact that the noise spectrum is narrower than the oscilloscope bandwidth and the occurrence of the spectrum peak indicates that the noise must have been transmitted through the target-–thus, it is not internal noise of the oscilloscope.

IV. Limitation of Spectrum of a Measured Pulse and Its Effect on Time Metrics

We will now assume that the measured currents of guns 1 and 2 are undistorted, full spectrum ESD pulses, and investigate in the same way as we did in Section II for theoretical pulses, how suppression of a high-frequency part of the spectrum by low-pass filtering affects the rise time and the peak current of the pulses in the time domain.

The effects of filtering with Butterworth filters of decreasing bandwidth are presented in Fig. 12 for a single pulse of gun 2, both in the time and in the frequency domain. For the 4- and 2-GHz bandwidths, the filtering suppresses in practice only the noise, so the pulse is only little distorted. Only for the 1-GHz bandwidth, the filtering removes a part of the spectrum emerging above the noise and smoothes the double peak. The time delay of the filtered pulse changes because the filter phase response is nonlinear-–it descends faster for a narrower bandwidth. For the linear phase filtering, the time delay is the same independent of the bandwidth. Since the recorded pulses are noisy, there is no point in considering changes of the time metrics after filtering

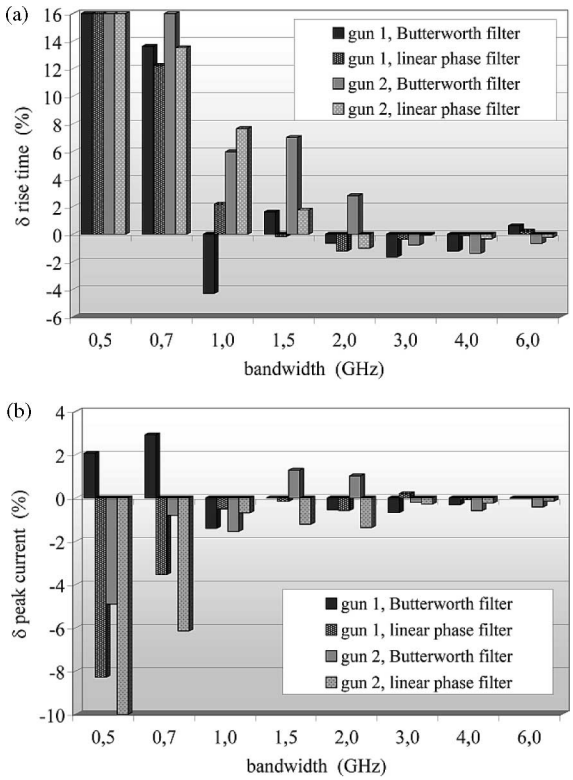

Fig. 13. Mean relative deviation of: (a) rise time (vertical scale is clipped); and (b) peak current versus the bandwidth of a pulse spectrum for series of measured pulses of guns 1 and 2.

TABLE II
RELATIVE DEVIATIONS OF TIME METRICS—MEASURED PULSES

Mean δ	Gun 1				Gun 2			
	Butterworth filter		linear phase filter		Butterworth filter		linear phase filter	
	2 GHz	3 GHz	2 GHz	3 GHz	2 GHz	3 GHz	2 GHz	3 GHz
δ_{rise_time} (%)	-0.65	-1.65	-1.22	-0.36	2.79	-0.79	-1.02	-0.09
δ_{peak_cur} (%)	-0.55	-0.68	-0.58	0.19	1.02	-0.20	-1.38	-0.28

for a single waveform—the results obtained for two particular pulses can be contrary to each other. Therefore, we evaluated $\delta_{\mathrm{rise\_time}}$ and $\delta_{\mathrm{peak\_current}}$ for each pulse and took their means for a whole series of recorded currents. The results, for the series of six pulses of gun 1 and the series of ten pulses of gun 2, are presented in Fig. 13.

The bar graphs indicate that to achieve reliable evaluation of the original (true) rise time and peak current, with maximum uncertainty below 3% and 1.5%, respectively (see Table II), a pulse bandwidth must not be restricted more than to 2 GHz. Reliable verification of guns producing rough pulses, with stronger high-frequency components, will require a wider bandwidth, in extreme cases, like that of gun 6 in Fig. 9—at least 4 GHz.

A too narrow measurement bandwidth typically stretches the rising slope. However, if the slope is stepped, like that of gun 6 in Fig. 9(a), restriction of the bandwidth smoothes it and leads, in a certain range, to decrease of the rise time calculated according to Standard [1]. Gun 6 produces pulses with multiple small peaks that merge after filtering into a single lower peak.

Another way of reducing the influence of noise in our analysis is averaging in time over a series of waveforms. A resulting time-averaged current preserves repeatable characteristics, whereas random details are suppressed (if we average, e.g., over ten pulses, the PSD of the averaged current noise will be reduced by 10 dBr/GHz). We computed such time-averaged currents for the series of pulses recorded for guns 1 and 2, filtered them as original undistorted pulses, and compared the time metrics before and after filtering. The results are very similar to those presented in Fig. 13, which validates our conclusion.

V. CONCLUSION

On the basis of the presented results, we can state that a measurement path (including an oscilloscope) with a 3-GHz bandwidth is sufficient to neglect frequency distortions for the steepest theoretical pulse with a 0.6-ns rise time. The deviation of the metrics due to limitation of a pulse spectrum is below 1.5% for the rise time and 0.1% for the peak current (see Table I). For a typical slower pulse, with a 0.8-ns rise time, a 2-GHz bandwidth is wide enough.

As to real ESD pulses, if they are relatively smooth, like the pulses of guns 1 or 2 (see Figs. 7 and 10), the main component of their spectra above 3 GHz is the noise. The source of this noise is the gun's discharge switch. Most manufacturers of ESD guns use the same HV 35-kV vacuum or SF-6/N2 filled relays, therefore, the level of the noise is more or less the same for each gun. If the spectrum of a real pulse is limited to below 2 GHz, it is distorted in the same way as a clean theoretical pulse. A too narrow bandwidth, especially less than 1.5 GHz, can easily result in incorrect evaluation of the metrics and erroneous verdict of verification. When a setup bandwidth is greater than 2 GHz, the main source of the measurement uncertainty becomes the pulse noise. For a 3-GHz bandwidth, the uncertainty is about 1.65% for the rise time and 1.4% for the peak current (mean deviations averaged over series of pulses, see Table II). The deviations in Fig. 13, especially for the rise time, do not diminish to zero with increase of the filter bandwidth, because the filters are not "transparent" for the noise. Obviously, the influence of the noise can be reduced by averaging measured metrics over a series of pulses. Even though a 3-GHz bandwidth setup does not ensure distortion-free (in the sense we defined) transmission of a pulse, the frequency-dependent contribution is only about 20% of the allowable expanded uncertainty. Further expansion of an oscilloscope bandwidth will not reduce the deterministic component of the uncertainty. As far as the authors know, the noise component has not yet been taken into account in calculating the uncertainty in ESD verification. However, a more detailed analysis of this issue goes beyond the scope of this paper.

Verification of guns that produce rough pulses, with steps on the rising slope and/or several smaller peaks (see Fig. 9), whose high-frequency part of the spectrum above 3 GHz contains distinctive resonance peaks emerging above the noise level, requires a wider bandwidth—4 GHz or even more.

For a given bandwidth, the more linear is the frequency phase response of a measurement path, the smaller is distortion of a pulse due to restriction of its spectrum. The rise time is a metric most sensitive to restriction of the spectrum and nonlinearity of the phase shift.

ACKNOWLEDGMENT

The authors would like to thank Prof. D. Pommerenke and his research group, particularly Dr. J. Koo, Missouri University of Science and Technology, for making available the results of round robin tests and consulting, and also Prof. O. Fujiwara, Nagoya Institute of Technology, and his research group, in particular Dr. Y. Taka, for making available measurement data recorded with a 12-GHz oscilloscope.

REFERENCES

[1] *Electromagnetic Compatibility (EMC)—Part 4–2: Testing and Measuring Techniques—Electrostatic Discharge Immunity Test*, IEC 61000-4-2, Dec. 2008.

[2] *International Standard: Information Technology Equipment—Safety—Part 1: General Requirements*, IEC 60950-1, Dec. 2005.

[3] J. Baran and J. Sroka, "Uncertainty of ESD pulse metrics due to dynamic properties of oscilloscope," *IEEE Trans. Electromagn. Compat.*, vol. 50, no. 4, pp. 802–809, Nov. 2008.

[4] C. Mittenmayer and A. Steininger, "On the determination of dynamic errors for rise time measurement with an oscilloscope," *IEEE Trans. Instrum. Meas.*, vol. 48, no. 6, pp. 1103–1107, Dec. 1999.

[5] Y. Taka, T. Adachi, O. Fujiwara, S. Ishigami, and Y. Yamanaka, "Reconstruction of discharge currents injected on calibration target from electrostatic discharge generator," in *Proc. 18th Int. Symp. Electromagn. Compat. (EMC)*, Zurich, Switzerland, Sep.2007, pp. 349–352.

[6] K. Kawamata, S. Minegishi, Y. Taka, and O. Fujiwara, "A method for estimating wideband transients using transmission loss of high performance semi-rigid coaxial cable," *IEICE Trans. Commun.*, vol. E92-B, no. 6, pp. 1965–1968, Jun. 2009.

[7] J. Koo, Q. Cai, K. Wang, J. Maas, T. Takahashi, A. Martwick, and D. Pommerenke, "Correlation between EUT failure levels and ESD generator parameters," *IEEE Trans. Electromagn. Compat.*, vol. 50, no. 4, pp. 794–801, Nov. 2008.

Janusz Baran was born in Czestochowa, Poland, in 1961. He received the M.Sc. degree in electrical engineering from Czestochowa University of Technology, Czestochowa, Poland, in 1985, and the Ph.D. degree in electrical engineering from the Lublin University of Technology, Lublin, Poland, in 1990.

Since 1986, he has been with the Institute of Electronics and Control Systems, Czestochowa University of Technology. His current research interests include signal processing, digital control, and adaptive systems.

Jan Sroka (M'01–SM'05) was born in Szczerców, Poland, in 1952. He received the M.Sc., Ph.D., and D.Sc. degrees in electrical engineering from the Warsaw University of Technology, Warsaw, Poland, in 1974, 1982, and 1990, respectively.

From 1991 to 1994, he was with the Group of Electromagnetic Fields, Federal Institute of Technology, Zürich, Switzerland. In 1995, he was with Schaffner EMC AG, Switzerland, where he was at different departments: Research and Technology; Components Development; and Test Systems Development. Since 2006, he has been with EMC-Testcenter Zürich AG, Switzerland. He is also a Research Coworker at the Institute of Theoretical Electrical Engineering and Systems, Warsaw University of Technology. His current research interests include investigation of the electrostatic discharge phenomenon as well as establishment of uncertainty budget in electromagnetic compatibility calibration and testing.